Journal of Organometallic Chemistry, 444 (1993) 83–89

JOM 23070

Synthesis and reactivity of substituted cyclopentadienyl diphenylphosphido complexes of zirconium(IV). X-Ray crystal structure of $[(C_5H_4SiMe_3)_2Zr(PPh_2)_2]$

Anne-Marie Larsonneur and Robert Choukroun

Laboratoire de Chimie de Coordination du CNRS, UPR 8241 liée par conventions à l'Université Paul Sabatier et à l'Institut National Polytechnique, 205 route de Narbonne, 31077 Toulouse Cedex (France)

Jean-Claude Daran

Laboratoire de Chimie des Métaux de Transition, Université Pierre et Marie Curie, 75230 Paris Cedex 05 (France)

Tomas Cuenca, Juan Carlos Flores and Pascual Royo

Departamento de Quimica Inorganica, Facultad de Ciencias, Universidad de Alcalà de Henares, 28871 Alcalà de Henares Madrid (Spain)

(Received May 13, 1992)

Abstract

The syntheses of $[(C_5H_4SiMe_3)_2Zr(PPh_2)_2]$ (1) and $[(C_5H_5)(C_5Me_5)Zr(PPh_2)_2]$ (2) are described. The X-ray crystal structure of 1 has been determined (monoclinic, $P2_1/n$; $a = 17.951(8)$; $b = 23.776(11)$; $c = 9.163(10)$ Å; $\beta = 99.29(6)°$; $Z = 4$) and it contains two distinct types of phosphido-ligands. Cyclic voltammetry measurements and chemical reduction of 1 are described, and the monophosphido Zr^{III} adduct species, $[(C_5H_4SiMe_3)_2Zr(PPh_2)(PhC{\equiv}CH)]$ identified by electron spin resonance spectroscopy. Reaction of 1 with the rhodium complex $[Rh_2(\mu\text{-}S\text{-}{}^tBu)_2(CO)_4]$ affords the heterometallic complex $[\{C_5H_4SiMe_3)_2Zr(\mu\text{-}PPh_2)_2(Rh(\mu\text{-}S\text{-}{}^tBu)_2Rh)(\mu\text{-}PPh_2)_2Zr(C_5H_4SiMe_3)_2]$ (3). The catalysis of the hydroformylation of 1-hexene with 3 as catalyst has been investigated.

1. Introduction

In the vast amount of work devoted to heterobimetallic complexes, and particularly to complexes containing early electron-deficient and late electron-rich metal centres [1], our interest has focussed on systems able to perform hydroformylation catalysis using the cooperative effect of a [Zr,Rh] or [Ti,Rh] system. We have demonstrated the ability of the diphenylphosphinomethyl ligand σ-bonded to zirconium (or titanium) to form bimetallic complexes and we have carried out systematic studies of these systems in hydroformylation reactions [2].

A recent report of Stephan *et al.* [3] has shown the catalytic activity of a bimetallic system, $[(C_5H_5)_2Zr(\mu\text{-}PPh_2)_2RhH(CO)(PPh_3)]$, in the hydroformylation of 1-hexene, with a significant selectivity for the terminal aldehyde.

In an attempt to check whether a phosphidozirconium complex associated with the dinuclear rhodium complex $[Rh_2(\mu\text{-}S\text{-}{}^tBu)_2(CO)_4]$ could increase the hydroformylation rate and selectivity, we synthesised the substituted cyclopentadienylphosphidozirconium complexes $[(C_5H_4SiMe_3)_2Zr(PPh_2)_2]$ (1) and $[(C_5H_5)(C_5Me_5)Zr(PPh_2)_2]$ (2). The chemical reactivity, cyclic voltammetry, and chemical reduction of 1 and 2 have been investigated, as well as the hydroformylation catalysis of 1-hexene with 1 in the presence of $[Rh_2(\mu\text{-}S\text{-}{}^tBu)_2(CO)_4]$ and $[RhH(CO)(PPh_3)_3]$.

Correspondence to: Dr. R. Choukroun or Dr. P. Royo.

0022-328X/93/$6.00

$$[(C_5H_4SiMe_3)_2ZrCl_2] + 2LiPPh_2 \longrightarrow \underset{(\mathbf{1})}{[(C_5H_4SiMe_3)_2Zr(PPh_2)_2]} + 2LiCl$$

$$[(C_5H_5)(C_5Me_5)_2ZrCl_2] + 2LiPPh_2 \longrightarrow \underset{(\mathbf{2})}{[(C_5H_5)(C_5Me_5)_2Zr(PPh_2)_2]} + 2LiCl$$

Scheme 1.

2. Results and discussion

2.1. Synthesis and spectroscopic data for $[(C_5H_4SiMe_3)_2Zr(PPh_2)_2]$ (1) and $[(C_5H_5)(C_5Me_5)Zr(PPh_2)_2]$ (2)

Treatment of a toluene solution of $[(C_5H_4SiMe_3)_2ZrCl_2]$ or $[(C_5H_5)(C_5Me_5)ZrCl_2]$ with stoichiometric amount of $LiPPh_2$ resulted in a dark solution which, after work up, afforded black crystals of **1** (yield 60%) and black-blue crystals of **2** (yield 90%).

The ^1H and ^{13}C NMR spectra were assigned unambiguously. The $^{31}P\{^1H\}$ NMR spectra of **1** and **2** show a single low-field resonance at 144.1 and 117.5 ppm, respectively. No change was observed down to $-90°C$. This compares with $[(C_5H_5)_2Hf(PPh_2)_2]$ [4] and $[\{C_5H_3(SiMe_3)_2\}_2Zr\{P(Ph)C_6H_4P(Ph)\text{-}1,2\}]$ [5] where two ^{31}P signals were observed at low temperature, indicating two different conformations about the phosphorus atoms, and confirmed by X-ray structures [4,5] showing one phosphorus atom with a pyramidal geom-

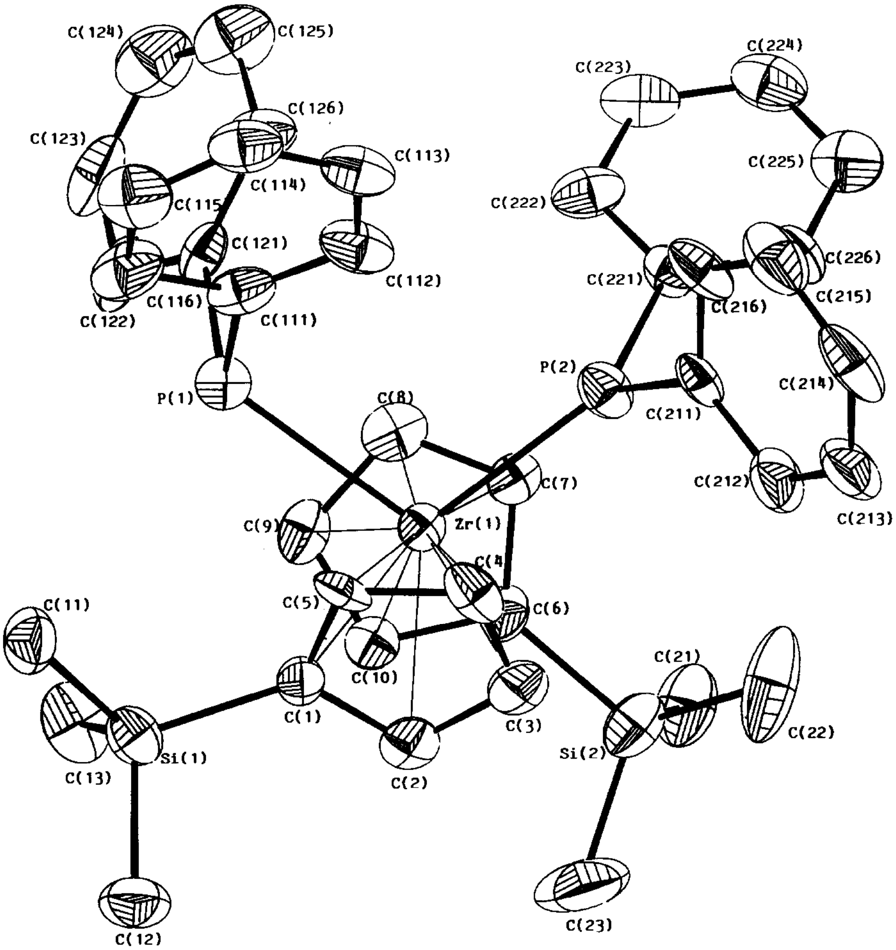

Fig. 1. An ORTEP view of the structure of $[(C_5H_4SiMe_3)_2Zr(PPh_2)_2]$ (1); hydrogen atoms are omitted for clarity.

etry while the other is planar, indicative of a p_π–d_π ligand-to-metal bonding.

The observation of a single resonance in the ^{31}P NMR spectra of **1** and **2** gives no information about the environment of the phosphorus atoms because equilibration between two kinds of phosphorus atoms is possible via a rapid fluxional process on the NMR time scale.

2.2. *X-Ray crystal structure of 1*

Details of the crystal structure determination are provided in the experimental section. Figure 1 shows an ORTEP perspective of the molecular structure of **1**. Selected bond distances and bond angles are listed in Table 1. The molecule exhibits a pseudo-tetrahedral geometry with angles ranging from 135.45(4)° (ring centroid–Zr–ring centroid) to 99.52(6)° (ring centroid (1)–Zr–P(1), the remaining three angles being 105.65(6)° (centroid(1)–Zr–P(2)), 105.28(7)° (ring centroid(2)–Zr–P(2)), and 103.38(6)° (ring centroid(2)–Zr–P(1)).

The most remarkable features concern the geometry around the phosphorus atoms, P(1) and P(2), *viz.* a pyramidal geometry around P(1) (the sum of the angles at P(1) is 326.6°) while the geometry around P(2) is trigonal planar (the sum of the angles at P(2) is 360°), corresponding to a shorter Zr–P(2) bond (2.536(3) Å) than the Zr–P(1) bond (2.694(3) Å). This is consistent with a double bond between Zr and P(2).

2.3. *Electrochemical and chemical reduction*

The redox potentials of $[(C_5H_4SiMe_3)_2ZrCl_2]$ [6] and $[(C_5H_5)(C_5Me_5)ZrCl_2]$ are $E_{1/2} = -1.59$ and -1.77 V *vs.* SCE, respectively. Compound **1** undergoes a quasi reversible electron-transfer reaction at a scan rate of 2 V s^{-1} (Pt electrode, 10^{-1} mol l^{-1} NBu_4BF_4, THF solution). The ratio of the peak current is $i_a/i_c = 0.7$ ($i_a/i_c \equiv i_{anodic}/i_{cathodic}$) with a formal potential $E_{1/2} = -1.72$ V and a peak-to-peak separation $\Delta E_p = 183$ mV. The reversibility decreases when the scan rate decreases and the calculated values of the half-life order are close to 2 s at room temperature for the reduced species observed in the cyclic voltammogram. Cyclic voltammetry of **2** shows two reductive waves: the first at $E_{1/2} = -1.65$ V is reversible at a scan rate of 2 V s^{-1} ($i_a/i_c = 0.9$; $\Delta E_p = 123$ mV) while the second wave at -2.83 V is less well defined.

Unfortunately, the black THF solutions of **1** or **2** are extremely moisture-sensitive which precludes ESR measurements using controlled potential electrolysis under our experimental conditions.

The chemical reduction of **1** with 1 equiv. of sodium dihydronaphthalenide Na(np) in THF at room temperature produces thermally stable Zr^{III} species, demonstrated by a unique, intense ESR signal ($g = 1.986$; $a(^{91}Zr) = 24$ G; $\Delta B = 5$ G) (Fig. 2(a)).

The chemical reduction of similar analogous species $[Cp_2M(PR_2)_2]$ gives a typical ESR spectrum with a doublet for $[Cp_2M(PR_2)]$, a 1 : 2 : 1 triplet for $[Cp_2M(PR_2)_2]^-$ and a quartet of 1:2:1 triplets for $Na[[(Cp_2M(PR_2)_2]$ [4,7,8]. Reduction of **1** with other reductants such as Li(np) and K(np) gives the same ESR feature as observed with **1** and Na(np), which proves the absence of alkali metal splitting. In attempts to elucidate the ESR signal, ^{31}P NMR experiments of the different solutions were recorded: at this stage, the ^{31}P NMR spectra show the presence of $LiPPh_2$ (-23 ppm), $KPPh_2$ (-9.1 ppm) and PPh_2PPh_2 (-15 ppm) when the reduction is performed with Li(Np), K(np), and Na(np), respectively, with the simultaneous presence of another unattributed peak at -110 ppm. Addition of CH_3I gives the phosphonium salt $[PPh_2Me_2]I$ ($\delta = 21$ ppm) exclusively.

We attempted to identify this Zr^{III} species through its reactivity with alkynes [9]. Addition of diphenylacetylene to a solution of (**1** + Na(np)) did not change the ESR spectrum, but adding PhC≡CMe and PhC≡CH in an excess gave a doublet and a doublet of doublets, respectively, suggesting the formation of monophosphidozirconium(III) species $[(C_5H_4SiMe_3)_2Zr(PPh_2)(PhC{\equiv}CMe)]$ ($g = 1.983$; $a(^{31}P) = 19.2$ G) and $[(C_5H_4SiMe_3)_2Zr(PPh_2)(PhC{\equiv}CH)]$ (Fig. 2b) ($g = 1.983$; $a(^{31}P) = 19.5$ G; $a(^1H) = 4.3$ G; $a(^{91}Zr) = 10$ G). The ESR signal of the phenylacetylene adduct was confirmed with deuterated PhC≡CD, and consisted of a doublet with (**1** + Na(np)) (Fig. 2(c)) with the same

TABLE 1. Interatomic distances (Å) and bond angles (°) for non-hydrogen atoms of $[(C_5H_4SiMe_3)_2Zr(PPh_2)_2]$; e.s.d.s in parentheses refer to the last significant digit; CEN refers to the centre of a $C_5H_4SiMe_3$ ring

Zr(1)–CEN(1)	2.2060(8)	CEN(1)–Zr(1)–CEN(2)	135.45(4)	P(2)–Zr(1)–P(1)	103.75(9)
Zr(1)–CEN(2)	2.2031(8)	CEN(1)–Zr(1)–P(1)	99.52(6)	C(111)–P(1)–Zr(1)	113.2(3)
Zr(1)–P(1)	2.694(3)	CEN(1)–Zr(1)–P(2)	105.65(6)	C(121)–P(1)–Zr(1)	113.8(3)
Zr(1)–P(2)	2.536(3)	CEN(2)–Zr(1)–P(1)	103.38(6)	C(121)–P(1)–C(111)	99.5(4)
P(1)–C(111)	1.86(1)	CEN(2)–Zr(1)–P(2)	105.28(7)	C(211)–P(2)–Zr(1)	131.1(3)
P(1)–C(121)	1.848(9)			C(221)–P(2)–Zr(1)	125.6(3)
P(2)–C(211)	1.793(9)			C(221)–P(2)–C(211)	103.2(4)
P(2)–C(221)	1.802(9)				

hyperfine coupling constants as for the analogous phenylacetylene adduct, the magnitude of $a(^2D)$ being small enough to prevent resolution of the ^2D coupling ($a(^2D) = 1/6\ a(^1H)$) ($g = 1.981$; $a(^{31}P) = 19.2$ G; $a(^{91}Zr = 10$ G); $\Delta B = 2$ G). CH_3I was also added to a THF solution containing a mixture of **1**, Na(np) and PhC≡CH in an excess, to ensure that the observed doublet of doublets of the reduced species is not due to a Zr^{III} hydride species, which is easily accessible in Zr^{III} chemistry [10]. No evolution of methane was identified by IR analysis, excluding the formation of a hydride.

2.4. [Zr,Rh] heterometallic complexes: synthesis and catalytic activity in hydroformylation

Upon adding the dinuclear rhodium complex $[Rh_2(\mu\text{-S-}^tBu)_2(CO)_4]$ to **1** in THF under a partial vacuum to evolve CO gas, the heterometallic complex $[(C_5H_5SiMe_3)_2Zr(\mu\text{-PPh})_2\{Rh(\mu\text{-S-}^tBu)_2Rh\}(\mu\text{-PPh}_2)_2Zr(C_5H_4SiMe_3)_2]$ (**3**) was formed. Both the IR and the ^{13}C NMR spectrum show the absence of CO (by comparison with $[(Cp\text{-}^tBu)_2Zr(CH_2PPh_2)_2Rh(S\text{-}^tBu)_2(CO)_2]$ [2a]: ν(CO) 1947, 1930 cm^{-1}; $\delta(^{13}CO)$194.2 ppm, $J_{Rh-C} = 77$ Hz, $J_{P-C} = 11$ Hz). ^1H and ^{13}C NMR spectra show the equivalences of the proton and carbon resonances (single $SiMe_3$, ^tBu resonances and one type of phenyl environment). The ^{31}P NMR spectrum (at 101.26 and 36.43 MHz) shows two resonances at 176.3 ppm ($J_{Rh-P} = 90$ Hz, $J_{P-P} = 13$ Hz) and 183.9 ppm ($J_{Rh-P} = 70$ Hz, $J_{P-P} = 13$ Hz) and no dynamic process on the ^{31}P NMR time scale is observed over the temperature range 373–193 K in toluene-d_8, indicating a rigid and a non-symmetric structure for **3** and a *cis* position for the phosphorus atom bonded to the same rhodium atom, as revealed by the low J_{P-P} coupling. Unfortunately, attempts to prepare suitable crystals for an X-ray structure determination have failed, but Scheme 2 shows the proposed scheme for the formation of **3**, based on the spectroscopic data (Fig. 3):

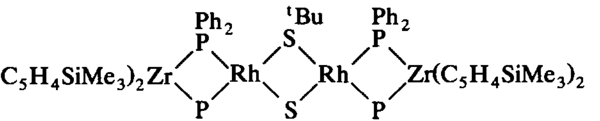

(3)

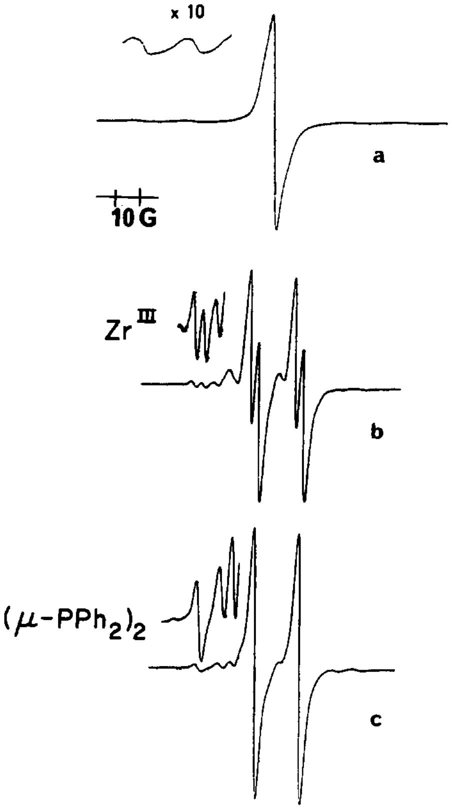

Fig. 2. Observed solution EPR spectra (in THF) and expanded view (×10) for a portion of the Zr hyperfine signals (^{91}Zr, 11.3% natural abundance, $I = 5/2$): (a) **1** + Na(np); (b) **1** + Na(np) in the presence of PhC≡CH; (c) **1** + Na(np) in the presence of PhC≡CD.

We nevertheless used **3** in the hydroformylation of 1-hexene at 80°C under 20 bar pressure (H_2/CO 1:1) with a 1:400 catalyst/substrate ratio in THF. The reaction was monitored by GC. A very slow rate of conversion of 1-hexene to aldehydes was observed with a linear-to-branched isomer ratio $n = 2.3$ (90% conversion in 17 h). By comparison with our previous results for $[Cp_2Zr(CH_2PPh_2)_2]$ and various Rh complexes [2], 2–3 h were necessary to convert 95% of 1-hexene with roughly the same linear/branched ratio n.

Remembering that $[Cp_2Zr(PPh_2)_2\{RhH(CO)PPh_3\}]$ [3] shows under 1 bar 1:1 H_2/CO pressure at 25°C, a linear/branched selectivity $n = 16$ for a nearly total conversion of 1-hexene within 100 h, we have performed the catalytic hydroformylation reaction under similar experimental conditions with a stoichiometric mixture of **1** and $[RhH(CO)(PPh_3)_3]$. The ^{31}P NMR spectrum of the mixture was first registered to ascertain the *in situ* formation of the bimetallic complex $[(C_5H_4SiMe_3)_2Zr(\mu\text{-PPh}_2)_2\{RhH(CO)(PPh_3\}]$ (AB_2X

$$\mathbf{1} + [Rh_2(\mu\text{-S-}^tBu)_2(CO)_4] \longrightarrow \underset{(3)}{\{(C_5H_4SiMe_3)_2Zr(PPh_2)_2\}_2Rh_2(\mu\text{-S-}^tBu)_2} + 4CO$$

Scheme 2.

system, $\delta_{P_A} = 42.43$ ppm, dt; $J_{Rh-P} = 138$ Hz; $\delta_{P_B} = 121.15$ ppm, dd; $J_{Rh-P} = 96$ Hz; $J_{P_A-P_B} = 17$ Hz and free phosphine PPh_3, $\delta = -5.0$ ppm). These values are similar to those obtained with the analogous $[Cp_2Zr(\mu\text{-}PPh_2)_2RhH(CO)(PPh_3)]$. This mixture gives complete conversion of 1-hexene (99%) to aldehydes within 55 h and the selectivity reached is $n = 10$. The ^{31}P NMR spectrum of the solution shows that the bimetallic system remains intact after catalysis. Although the catalytic hydroformylation rate has increased upon addition of an $SiMe_3$ group to a cyclopentadienyl ligand, this modification is less favourable in terms of selectivity when compared to the results obtained with $[Cp_2Zr(\mu\text{-}PPh_2)_2RhH(CO)(PPh_3)]$.

3. Conclusion

By comparison with the unsubstituted cyclopentadienyl analogue, the different behaviour of **1** is mainly in its chemical reduction and the influence of the $SiMe_3$ group (steric and/or electronic [4]). The alkyne monophosphido-adducts $[(C_5H_4SiMe_3)_2Zr(PPh_2)(PhC{\equiv}CR)]$ (R = Me or H), are formulated based on ESR spectroscopy, and this species may result from $[(C_5H_4SiMe_3)_2Zr(PPh_2)]$ as the first step of the chemical reduction of **1**.

Complex **3** is a poor catalyst for hydroformylation, by comparison with other diphenylphosphinomethyl zirconium complexes containing rhodium, and this may be due to the absence of sites necessary to bind H_2 and/or CO. The active catalytic solution of **1** and $[RhH(CO)(PPh_3)_3]$ under mild conditions provides evidence for the influence of the electron acceptor $SiMe_3$ group on the hydroformylation rate when compared to previous work by Stephan *et al.*, but with a decrease in the selectivity in our case.

4. Experimental details

All manipulations were carried out under an inert atmosphere (argon) by conventional Schlenk tube techniques or using a dry box (Vacuum Atmosphere Dri-Lab) filled with dinitrogen. Liquids were transferred via syringe or cannula. ^1H, ^{13}C and ^{31}P NMR spectra were recorded on a Bruker 250 spectrometer. ESR spectra were recorded on a Bruker 200TT spectrometer. Elemental analyses were performed by the Service Central de Microanalyse du CNRS.

A home made microcomputer-controlled instrument with ohmic resistance compensation was used for cyclic voltammetry studies. A platinum auxiliary electrode and an SCE reference electrode were used in conjunction with a platinum disk electrode as working electrode.

NBu_4PF_6 was used as supporting electrolyte for cyclic voltammetry studies. It was melted under vacuum before use to ensure efficient dehydration. $PhC{\equiv}CD$ was prepared by hydrolysis of $LiC{\equiv}CPh$ with D_2O and its formulation confirmed by mass spectra ($m/e = 103$) and ^1H NMR spectroscopy (absence of the ethylenic proton). $LiPPh_2$, $[(C_5H_4SiMe_3)_2ZrCl_2]$, $[(C_5H_5)(C_5Me_5)ZrCl_2]$, $[Rh_2(\mu\text{-}S\text{-}{}^tBu)_2(CO)_4]$, and $[RhH(CO)(PPh_3)_3]$ were prepared by published procedures [11–14].

4.1. Preparation of $[(C_5H_4SiMe_3)_2Zr(PPh_2)_2]$ (1)

Treatment of a suspension of $[(C_5H_4SiMe_3)_2ZrCl_2]$ (3.50 g, 8.02 mmol) in toluene (20 ml) with 2 equiv. of $LiPPh_2$ (3.08 g, 16.04 mmol) in toluene (10 ml) at room temperature afforded a dark purple solution. The solution was filtered to remove LiCl, reduced to 10 ml, and layered with hexane. Microcrystals of **1** were separated by filtration. ^1H NMR (C_6D_6): δ 6.04, 6.08 (m, C_5H_4); 0.17 (s, $SiMe_3$); 7.78, 7.15, 7.02 (m, C_6H_5) ppm. $^{31}P\{^1H\}$ NMR ($C_6D_5CD_3$), referenced to H_3PO_4 in D_2O: δ 144.1 (s) ppm. ^{13}C NMR (C_6D_6): δ 115.40 (s, substituted C, C_5H_4); 115.99 (d, $J_{CH} = 107$ Hz, C_5H_4); 111.16 (d, $J_{CH} = 170$ Hz, $J_{CP} = 6.4$ Hz, C_5H_4); 0.47 (s, $J_{CH} = 120$ Hz, $SiMe_3$); 146.55 (s, C_6H_5); 135.28, 126.70, 128.11 (d, $J_{CH} = 160$ Hz, C_6H_5) ppm. Yield: 3.5 g (60%). Anal. Found: C, 64.61; H, 6.33; Zr, 12.2. $C_{40}H_{46}P_2Si_2Zr$ calc.: C, 65.31; H, 6.26; Zr, 12.41%.

4.2. Preparation of $[(C_5H_5)(C_5Me_5)Zr(PPh_2)_2]$ (2)

A suspension of $[(C_5H_5)(C_5Me_5)ZrCl_2]$ (2.04 g, 5.63 mmol) in toluene (50 ml) was added to a suspension of $LiPPh_2$ (2.16 g, 11.26 mmol) at room temperature. The reaction mixture changed immediately from yellow to black-blue. The mixture was stirred for 30 min. After filtration the resulting solution was evaporated to dryness. Extraction with 100 ml of a toluene/hexane mixture (50%) gave a solution which was evaporated to 30 ml under vacuum. Cooling to −30°C produced the compound as a black-blue crystalline solid (2.73 g, 4.13 mmol). From the mother liquor, a second fraction was obtained (0.63 g, 0.95 mmol) (90% yield). ^1H NMR: δ 1.71 (s, 15H, C_5Me_5); 5.65 (s, 5H, C_5H_5); 7.01–7.17 (m, Ph) ppm. ^{13}C NMR (C_6D_6): δ 12.80 [s, $C_5(CH_3)_5$]; 108.18 (s, C_5H_5); 119.12 [s, $C(CH_3)_5$]; 126.44–146.50 (Ph) ppm. $^{31}P\{^1H\}$ NMR (C_6D_6), referenced to H_3PO_4 in D_2O): δ 117.53 (s) ppm. Anal. Found: C, 71.13; H, 6.16. $C_{39}H_{40}P_2Zr$ calc.: C 70.78; H, 6.05%.

4.3. Chemical reduction of *1*

All experiments were performed in a Vacuum Atmosphere Dri-Lab. In a typical procedure, *1* (60 mg, 0.081 mmol) in 0.5 ml of THF was treated with 1 equiv. of a THF solution of sodium dihydronaphthalenide (prepared from a mixture of naphthalene (11 mg, 0.081 mmol) and an excess of sodium in 0.5 ml of THF with stirring for 2 h). The dark brown solution was stirred for 5 min and placed in NMR tubes with or without an excess of acetylene substrate. The tubes were sealed and the solutions monitored by ESR as well as ^{31}P NMR techniques. Solutions in sealed tubes were stable for weeks.

4.4. Preparation of $\{(C_5H_4SiMe_3)_2Zr(PPh_2)_2\}_2\{Rh_2(\mu\text{-}S\text{-}{}^tBu)_2\}$ *(3)*

$[Rh_2(S\text{-}\mu\text{-}{}^tBu)_2(CO)_4]$ (0.124 g, 0.25 mmol) in THF (10 ml) was added slowly to a THF solution of **1** (0.368 g, 0.5 mmol) at room temperature. The resulting solution was evacuated from time to time during addition of the rhodium solution to remove CO evolved. After addition, the solution was stirred for 1 h and evaporated to dryness. The resulting brown oil was extracted with hexane (40 ml), concentrated to 20 ml and left at room temperature for 24 h. A brown–red microcrystalline powder was separated from the solution. ^{1}H NMR (C_6D_6): δ 5.58, 5.12 (m, 16H, C_5H_4); 2.00 (s, 18H, CMe_3); 0.16 (s, 36H, $SiMe_3$); 8.2, 7.1 (m, 40H, C_6H_5) ppm. ^{31}P NMR (THF/C_6D_6): δ 176.3 (dd, $J_{Rh-P} = 90$ Hz, $J_{P-P} = 13$ Hz); 183.9 (dd, $J_{Rh-P} = 70$ Hz, $J_{PP} = 13$ Hz) ppm. ^{13}C NMR (C_6D_6): δ 111.1, 106.2, 105.5 (s, C_5H_4); 37.4 (q, $J_{CH} = 126$ Hz, CMe_3); 0.5 (q, $J_{CH} = 120$ Hz, $SiMe_3$); 142.2, 135.6, 134.4 (m, C_6H_5) ppm. Yield 0.230 g, 50%. Anal. Found: C, 58.5; H, 6.45; Zr, 9.65; Rh, 11.40. $C_{88}H_{110}P_4Rh_2Si_4S_2Zr_2$ calc.: C, 58.91; H, 6.14; Zr, 10.18; Rh, 11.49%.

TABLE 2. Crystallographic data for $[(C_5H_4SiMe_3)_2Zr(PPh_2)_2]$ (1) and structure determination details

Formula	$C_{40}H_{46}P_2Si_2Zr$
FW	736.1
System	Monoclinic
Space group	$P2_1/a$
a (Å)	17.951(8)
b (Å)	23.776(11)
c (Å)	9.163(10)
β (°)	97.29(6)
V (Å^3)	3879(46)
Z	4
μ(Mo-K_α) (cm^{-1})	4.45
$d_{calc.}$ (g cm^{-3})	1.26
2θ range (°)	$3 < 2\theta < 40$
Scan type	$\omega - 2\theta$
Scan width (°)	$1.0 + 0.34$ tg θ
Scan speed (° min^{-1})	0.9
Diffractometer	PhilipsPW1100
No. of reflections collected	4124
No. of unique reflections	3043
Merging factor	0.032
No. of reflections with $I > 3\sigma(I)$	2091
Absorption corrected by	DIFABS [16]
R	0.0513
R_w	0.0569
Weighting scheme [a]	$w = w'[1\text{-}(\Delta F/6\sigma(F))^2]^2$
Coeff. A_r for the Chebyshev serie	1.91; 0.50; 1.45
No. of variables	407

[a] $w' = 1/\Sigma_1{}^n A_r T_r(X)$ where n ($n = 4$) is the number of coefficients, A_r, for a Chebyshev polynomial series, for which X is $F_c/F_c(\max)$ [17].

TABLE 3. Fractional atomic coordinates with e.s.d.s in parentheses, and equivalent isotropic thermal parameter U_{eq} (Å^2)

Atom	x	y	z	U_{eq} [a]
Zr(1)	0.23230(5)	0.36185(4)	0.03981(9)	0.0422
P(1)	0.3750(1)	0.3945(1)	0.1240(3)	0.0545
P(2)	0.2454(2)	0.2607(1)	−0.0414(3)	0.0557
Si(1)	0.2376(2)	0.4782(1)	0.3551(3)	0.0598
Si(2)	0.0357(2)	0.3717(2)	−0.2104(4)	0.0740
C(1)	0.2129(5)	0.4049(4)	0.2848(9)	0.0474
C(2)	0.1432(6)	0.3871(4)	0.2123(9)	0.0551
C(3)	0.1400(5)	0.3286(5)	0.202(1)	0.0552
C(4)	0.2112(6)	0.3099(4)	0.268(1)	0.0524
C(5)	0.2533(5)	0.3552(4)	0.3187(9)	0.0480
C(6)	0.1366(5)	0.3917(4)	−0.168(1)	0.0507
C(7)	0.1972(5)	0.3677(4)	−0.2356(9)	0.0475
C(8)	0.2591(5)	0.4003(4)	−0.203(1)	0.0507
C(9)	0.2412(5)	0.4468(4)	−0.119(1)	0.0510
C(10)	0.1666(5)	0.4415(4)	−0.098(1)	0.0490
C(11)	0.3302(6)	0.4758(5)	0.469(1)	0.0745
C(12)	0.1627(6)	0.4983(6)	0.468(1)	0.0901
C(13)	0.2427(7)	0.5313(4)	0.210(1)	0.0786
C(21)	0.0077(7)	0.3882(6)	−0.409(1)	0.0996
C(22)	0.0240(9)	0.2942(6)	−0.175(2)	0.1033
C(23)	−0.0224(7)	0.4151(8)	−0.091(2)	0.1250
C(111)	0.4324(5)	0.3397(5)	0.232(1)	0.0571
C(112)	0.4245(6)	0.2829(5)	0.211(1)	0.0695
C(113)	0.4736(7)	0.2461(5)	0.294(1)	0.0772
C(114)	0.5292(6)	0.2668(6)	0.396(1)	0.0718
C(115)	0.5350(7)	0.3220(6)	0.424(1)	0.0886
C(116)	0.4872(6)	0.3602(5)	0.341(1)	0.0786
C(121)	0.4313(5)	0.4032(4)	−0.0301(9)	0.0475
C(122)	0.4365(6)	0.4556(5)	−0.093(1)	0.0669
C(123)	0.4788(6)	0.4661(5)	−0.209(1)	0.0699
C(124)	0.5168(7)	0.4217(7)	−0.262(1)	0.0954
C(125)	0.5145(7)	0.3698(6)	−0.199(1)	0.0902
C(126)	0.4724(5)	0.3598(5)	−0.087(1)	0.0670
C(211)	0.2380(6)	0.1956(4)	0.0551(9)	0.0491
C(212)	0.1692(6)	0.1770(4)	0.097(1)	0.0671
C(213)	0.1639(7)	0.1267(5)	0.170(1)	0.0831
C(214)	0.2246(9)	0.0937(4)	0.200(1)	0.0678
C(215)	0.2929(8)	0.1088(5)	0.159(1)	0.0838
C(216)	0.2980(6)	0.1597(4)	0.085(1)	0.0697
C(221)	0.2698(5)	0.2385(4)	−0.2172(9)	0.0468
C(222)	0.3259(6)	0.2653(4)	−0.284(1)	0.0665
C(223)	0.3437(6)	0.2492(5)	−0.419(1)	0.0701
C(224)	0.2347(6)	0.1926(4)	−0.291(1)	0.0570
C(225)	0.2533(6)	0.1761(5)	−0.427(1)	0.0809
C(226)	0.3072(7)	0.2018(5)	−0.493(1)	0.0769

[a] $U_{eq} = (U_{11}\ U_{22}\ U_{33})^{1/3}$

4.5. *General procedure for catalytic experiments*

Catalytic tests were carried out in a 75 ml autoclave. The temperature was maintained at 80°C or 25°C by oil circulation in a double jacket. The gas was admitted from a 125 ml bulb, and the drop of the pressure in the bulb was followed with a pressure gauge. Samples for GC analysis were syringed off during the course of the catalytic reaction.

4.6. *X-Ray crystal structure determination for $[(C_5H_4SiMe_3)_2Zr(PPh_2)_2]$ (1)*

4.6.1. *Collection and reduction of X-ray data*

Data were collected at room temperature on a Philips PW 1100 diffractometer. Unit cell parameters and basic information about data collection and structure refinement are given in Table 2. Accurate lattice parameters and orientation matrix were obtained from least-squares refinement of the setting angles of 25 well-centred reflections. The position of the Zr atom was determined by Harker vector analysis of three-dimensional Patterson maps. All remaining non-hydrogen atoms were located on successive difference electron density maps. The structure was refined by least-squares techniques with approximation (in three blocks) to the normal matrix using CRYSTALS [15]. All heavy atoms were refined anisotropically. H atoms were placed in calculated positions (H–C–H = 109°; H–C–C = 120°; C–H = 0.96 Å) and were not further refined but recalculated after each cycle. They were assigned isotropic thermal parameters 20% higher than those of C atoms to which they were attached. Anomalous dispersion terms were applied. Final positional and equivalent or isotropic temperature factors are listed in Table 3.

Supplementary data including hydrogen atom coordinates, anisotropic thermal parameters and structure factors are available from the authors.

Acknowledgments

We thank D. de Montauzon for pertinent discussions and the Action Intégrée France-Espagne (Grant No. 106-1989) for generous support to J.C.F. and A.M.L. and CICYT for financial support to Dept. Q. Inorganica (Project PB 89/0208).

References

1 (a) D. A. Roberts and G. L. Geoffroy, in G. Wilkinson, F. G. A. Stone and E. W. Abel (Eds.), *Comprehensive Organometallic Chemistry*, Pergamon, Oxford, 1982, Vol. 6, Chapter 40;
(b) D. W. Stephan, *Coord. Chem. Rev., 95* (1989) 41;
(c) R. T. Baker, W. C. Fultz, T. B. Morder and I. D. Williams, *Organometallics, 9* (1990) 2357 and refs. therein.

2 (a) R. Choukroun, F. Dahan, D. Gervais and C. Rifai, *Organometallics, 9* (1990) 1982 and refs. therein;
(b) A. M. Trzeciak, J. J. Ziolkowski and R. Choukroun, *J. Organomet. Chem.*, 420 (1991) 353.

3 L. Gelmini and D. W. Stephan, *Organometallics, 7* (1988) 849.

4 R. T. Baker, J.F. Whitney and S.S. Wreford, *Organometallics, 2* (1983) 1049;
L. Weber, G. Meine, R. Boose and N. Augart, *Organometallics, 6* (1987) 2484.

5 R. Bohra, P. B. Hitchcock, M. F. Lappert, M. F. and W. P. Leung, *J. Chem. Soc., Chem. Commun.*, (1989) 728.

6 M. F. Lappert, J. Pickett, P. I. Riley and P. I. Yarrow, *J. Chem. Soc., Dalton Trans.*, (1981) 805.

7 (a) J. G. Kenworthy, J. Myatt and P. Todd, *J. Chem. Soc., Chem. Commun.*, (1969) 263;
(b) J. G. Kenworthy, J. Myatt and P. Todd, *J. Chem. Soc. B.*, (1970) 792.

8 D. G. Dick and D. W. Stephan, *Organometallics, 10* (1991) 2811.

9 (a) E. Samuel, *Inorg. Chem.* 22 (1983) 2967; (b) J. L. Petersen and S. B. Jones, *Organometallics, 4* (1985) 966.

10 E. Samuel, *J. Am. Chem. Soc., 105* (1983) 1769.

11 S. R. Wade, M. G. H. Wallbridge and G. R. Willey, *J. Chem. Soc., Dalton Trans.*, (1983) 2555.

12 P. T. Wolczanski and J. W. Bercaw, *Organometallics, 1* (1982) 793.

13 P. Kalck and R. Poilblanc, *Inorg. Chem., 14* (1975) 2779.

14 D. Evans, G. Yagupski and G. Wilkinson, *J. Chem. Soc. A*, (1968) 2660.

15 D. J. Watkin, J. R. Carruthers and P. W. Betteridge, *CRYSTALS User's Guide*, Chemical Crystallography Laboratory, University of Oxford, Oxford, 1986.

16 N. Walker and D. Stuart, *Acta Crystallogr. Sect. A, 39* (1983) 158.

17 E. Prince, *Mathematical Techniques in Crystallography,* Springer, Berlin, 1982.